Available online at www.sciencedirect.com

ScienceDirect

IFAC Papers Online CONFERENCE PAPER ARCHIVE

IFAC PapersOnLine 55-34 (2022) 66–71

Fractional modeling of wind speed turbulence

Mohamed Hajjem [*,**] **Stéphane Victor** [*] **Patrick Lanusse** [*] **Pierre Melchior** [*] **Lara Thomas** [**]

[*] *Université de Bordeaux, IMS (UMR 5218 CNRS), Bordeaux Inp, 33405 Talence, France (e-mail: firstname.name@ims-bordeaux.fr).*

[**] *Safran Data Systems, 33260 La Teste-de-Buch, France (e-mail: firstname.name@safrangroup.com)*

Abstract: This paper proposes a method to design a wind turbulence model based on real wind spectral characteristics. It uses models based on Cole-Cole fractional functions to approximate the wind turbulence power spectral density. Von Kármán model is the most commonly used model but originally designed for aircraft in high altitude. Therefore, it is not suitable for systems operating at low altitude, hence the need for more accurate models in these specific conditions. Shaping filters issued from the fractional models are employed to generate realistic random wind speed turbulence from a random white noise input. Then, a grey box model is proposed from physical parameters such as the classic von Kármán ones (mean speed, turbulence intensity and length scale).

Keywords: Turbulence wind speed, Spectral analysis, Fractional model, Parameter estimation, Shaping filter, Real-time simulation

1. INTRODUCTION

Reducing the impact of wind disturbance on systems operating outdoors is an important consideration in system design. Models capable of accurately reproducing the behavior of wind turbulence are therefore required for system dynamics modeling and controller design. The study presented in this paper was conducted to improve the performance of mobile antennas used for tracking. Indeed, antennas are systems requiring a lot of precision, however wind turbulence increases the errors and the signal loss risks. The presented wind modeling can also be used in other fields. It is interesting for realistic dynamic behavior simulations of other systems than antennas: wind turbines (blades, mechanical forces, ...) (Feytout (2013)), wind response of solar panels, kites for traction or electric power generation (Cadalen et al. (2018b,a)), sailing, etc.

The design method presented in this paper is based on wind turbulence spectral characteristics because wind turbulence is a non-stationary stochastic process and consequently is difficult to model in time domain. These characteristics are described by the wind power spectral density (PSD) which will be approximated by models based on the well known von Kármán approximation (von Kármán (1948); Moorhouse and Woodcock (1982)) and on the Cole-Cole Cole and Cole (1941) fractional function. Cole-Cole functions have been widely used to model other diffusive phenomenon such as heat transfers in lungs (see Duhé et al. (2022)). Shaping filters designed from the wind PSD approximations will be able to generate random wind speed from a white noise input Diop et al. (2007).

A first study was proposed in Hajjem et al. (2021) where some rough approximations of the wind PSD were proposed by Cole-Cole and Davidson-Cole fractional PSD functions. Neither synthesis of shaping filters nor any time domain simulations were provided in Hajjem et al. (2021). After studying fractional shaping filters, a grey box model is proposed where the parameters can be adjusted according to the operating conditions.

This paper is organized as follows. Section 2 presents the von Kármán model and the results of its identification and its limitations. Then, section 3 proposes improved fractional models based on Cole-Cole fractional function. Section 4 presents the design of a grey box improved Cole-Cole model. Finally, a conclusion is drawn in section 5.

2. VON KÁRMÁN MODEL STUDY

2.1 von Kármán model

The wind speed can be represented as a sum of a steady component representing the mean speed related to the variations of the planetary weather and a fluctuating component representing the turbulence caused by topographic effects:

$$V(t) = \overline{V}(t) + V_{turb}(t), \tag{1}$$

where $\overline{V}(t)$ is the long-term component and $V_{turb}(t)$ the turbulence component. Van der Hoven (van der Hoven (1957)) explained this behavior by identifying two phases within the wind power spectrum. The turbulence phase contains an energy peak with a period around 75s. This paper will only focus on modeling this phase by the wind PSD approximation. Since the study concerns a short period of time, the mean wind speed will be considered constant.

10.1016/j.ifacol.2022.11.309

The modeling of the wind turbulence phase will be based on the von Kármán model (von Kármán (1948); Moorhouse and Woodcock (1982)). It is a non-integer order approximation of the linear and angular wind speed components PSD. It was developed by the United States Department of Defense based on earlier work by von Kármán for aircraft design and simulation applications. The wind speed PSD according to the von Kármán's longitudinal model is expressed as:

$$S(f) = \frac{4\sigma^2 \frac{L}{\overline{V}}}{\left(1 + 70.8(\frac{L}{\overline{V}}f)^2\right)^{5/6}}, \quad (2)$$

where f is the frequency, σ is the turbulence standard deviation, L is the length scale and $\overline{V}$ is the mean speed.

The von Kármán model is adjusted by the **length scale** L and the **turbulence intensity** I. The length scale represents the average size of a gust in appropriate directions and it is an important scaling factor in determining how rapidly gust properties vary in space. The turbulence standard deviation is expressed from the turbulence intensity by:

$$\sigma = I\overline{V}. \quad (3)$$

Mathematical models exist to estimate the values of L (ESDU (1985)) and I (IEC (2005) Ren et al. (2018)).

2.2 Shaping filters

Wind real-time simulation cannot be carried out directly from the PSD approximation. For this purpose, filters are employed to shape a random white noise at the input into an output that has the desired PSD, which in our case belongs to the wind turbulence. A shaping filter with a frequency response $H(f)$ will transform a white noise $x[n]$ into a signal of interest $y[n]$, namely:

$$Y(f) = H(f)X(f) \quad (4)$$

where $Y(f)$ and $X(f)$ respectively are the Fourier transforms (FT) of the output $y[n]$ and the input $x[n]$.

The white noise $x[n]$ at the input will have a constant PSD (S_{xx}) equal to its variance σ_x^2. Assuming that the input is a zero-mean and unitary variance white noise ($\sigma_x^2 = 1$), the output PSD (S_{yy}) can be expressed as:

$$S_{yy}(f) = S_{xx}(f)|H(f)|^2 = |H(f)|^2 = H(\mathrm{j}f)H^*(\mathrm{j}f), \quad (5)$$

where * denotes the conjugate operator.

In the case of wind turbulence modeling, the desired PSD is given by the expression of the von Kármán model, and therefore can be used to obtain the transfer function of a shaping filter, namely:

$$S_{VK}(f) = \frac{4\sigma^2 \frac{L}{\overline{V}}}{\left(1 + 70.8(\frac{L}{\overline{V}}f)^2\right)^{5/6}} = \frac{K}{(1 + (\tau f)^2)^{5/6}}, \quad (6)$$

where $K = 4\sigma^2 \frac{L}{\overline{V}}$ and $\tau = \sqrt{70.8}\frac{L}{\overline{V}}$.

The shaping filter issued from the von Kármán PSD approximation can be expressed as:

$$H_{VK}(\mathrm{j}f) = \frac{\sqrt{K}}{(1 + \mathrm{j}\tau f)^{5/6}} \quad (7)$$

where $H_{VK}(\mathrm{j}f)$ verifies (5).

2.3 Model identification

The reference for the model parameter identification is the PSD of one of the 28 wind speed datasets recorded next to the city of Montpellier, France. The studied signals have a period of 3 hours and a quasi-constant mean speed.

The nonlinear simplex algorithm (Subrahmanyam (1989)) is used to estimate the parameters of the von Kármán model. It will estimate the parameters K and τ of the von Kármán PSD expression (6) by minimizing the cost function corresponding to the normalized sum of the square errors between the measured PSD, S, and the estimated model, $\widehat{S}$, as:

$$J = \frac{1}{N}\sum_{i=1}^{N}\left|S_{dB}(f_i) - \widehat{S}_{dB}(f_i, K, \tau)\right|^2 \quad (8)$$

where N is the number of samples and f_i are the frequencies defined in the chosen frequency range.

The optimization is carried out in dB in order to maintain a better accuracy in the considered frequency range. Indeed, the PSD modulus is tending towards zero, thus leading to suboptimal optimization.

The estimated von Kármán model obtained on Matlab® is presented in Fig. 1.

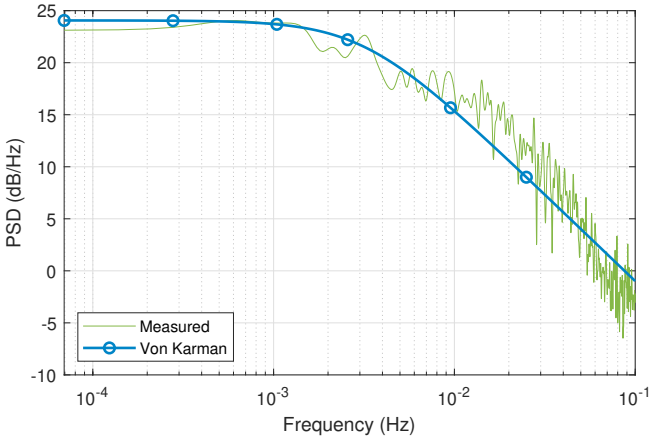

Fig. 1. Comparison between the estimated von Kármán PSD (–) and the measured wind PSD (–)

Fig. 1 shows that the von Kármán model provides a good fit in low frequencies. However, for $f > 0.01$Hz, the slope of the model seems to be different from the one of the measurements. The frequency range of wind turbulence is between 0.01Hz and 0.1Hz (van der Hoven (1957)) which corresponds to the range where the model is less accurate. This can be explained by the fact that the von Kármán model was originally designed for aircraft, and consequently for high altitudes and fast moving systems.

2.4 Model parameters

In this section, the von Kármán model estimated parameters K and τ (Fig. 2) are analyzed for all 28 datasets recorded next to the city of Montpellier, France.

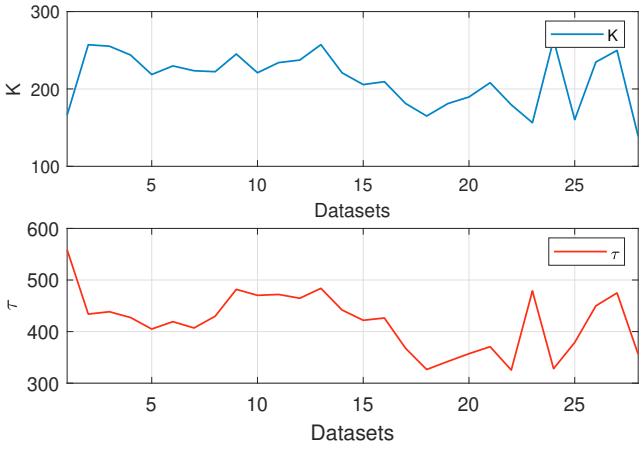

Fig. 2. The estimated parameters K and τ of the von Kármán model for different datasets

Both model parameters K and τ depend on the mean speed $\overline{V}$, the reference standard deviation σ and on the length scale L, and can be expressed as:

$$K = 4\sigma^2 \frac{L}{\overline{V}} \tag{9}$$

$$\tau = \sqrt{70.8}\frac{L}{\overline{V}} = 8.4\frac{L}{\overline{V}}. \tag{10}$$

$\overline{V}$ and σ are assumed known. As for L, it is very difficult to know its exact value because it depends on several factors, and at best, it can be approximated by mathematical models. The approximated value of the length scale from the ESDU model (ESDU (1985)) is:

$$L_{ESDU} = 25 z^{0.35} z_0^{-0.063} = 109.8m, \tag{11}$$

where $z = 40m$ is the measuring altitude and $z_0 = 0.05$ is a surface roughness parameter for open country.

Fig. 3 shows L_K and L_τ the length scale value calculated respectively from the estimated parameters K and τ. L_K directly stems from the von Kármán model gain (9) and therefore, the same coefficient 4 appears in the denominator.

$$L_K = \frac{K\overline{V}}{4\sigma^2} \tag{12}$$

On the other hand, L_τ, needs to be adjusted with a coefficient of 19.5 in order to be close to L_{EDSU} (11).

$$L_\tau = \frac{\tau\overline{V}}{19.5}. \tag{13}$$

The obtained values of L_K and L_τ vary between 80m and 130m with an average value of 106.4m for L_K and 109.2m for L_τ, thus, the two estimated parameters K and τ provide values very close to the approximated L_{ESDU}. The von Kármán model well estimates the gain K which provides directly accurate values of the length scale. Nevertheless, the coefficient $\sqrt{70.8}$ was too low to provide coherent values of the length scale. This means that the estimated time constant τ was too high.

3. FRACTIONAL MODEL APPROXIMATIONS

The von Kármán model which uses a non-integer order produces a fractional shaping filter whose differentiation

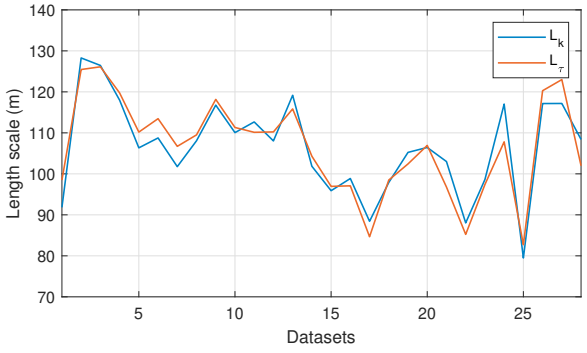

Fig. 3. Comparison between L_K the length scale value from K and L_τ obtained from τ

order is equal to $\nu = 5/6 \approx 0.833$. Fractional calculus has extended the possibilities of time and frequency identification by releasing the limit of the integer order. The Cole-Cole functions (Cole and Cole (1941)) are generally used to model complex systems with a reduced number of parameters (Sommacal (2007)). In order to improve the wind turbulence PSD estimation in high frequency, a new wind model based on the Cole-Cole fractional function form is introduced.

3.1 Cole-Cole based model

The slope obtained with von Kármán in high frequency is fixed by the non-integer order 5/6. However, according to the real data, this constraint can be released. Thus, the model fixed order will be replaced by an unknown parameter ν which will be estimated by the nonlinear simplex method, along with K and τ. The new model will be called the Cole-Cole (CC) model and its transfer function has the following expression:

$$H_{CC}(s) = \frac{\sqrt{K}}{1 + (\frac{\tau}{2\pi}s)^\nu}. \tag{14}$$

The PSD expression that will be identified is deduced from $H_{CC}(s)$ using equation (5):

$$\begin{aligned} \widehat{S}_{CC}(f) &= H_{CC}(\mathrm{j}f) H_{CC}(\mathrm{j}f)^* \\ &= \frac{\sqrt{K}}{1 + (\mathrm{j}\tau f)^\nu} \frac{\sqrt{K}}{1 + (-\mathrm{j}\tau f)^\nu} \\ &= \frac{K}{(1 + (\mathrm{j}^\nu + (-\mathrm{j})^\nu)(\tau f)^\nu + (\tau f)^{2\nu})}. \end{aligned} \tag{15}$$

The expression of the Cole-Cole model PSD, $\widehat{S}_{CC}(f)$, is then:

$$\widehat{S}_{CC}(f) = \frac{K}{1 + 2\cos(\nu\frac{\pi}{2})(\tau f)^\nu + (\tau f)^{2\nu}}. \tag{16}$$

Fig. 4 presents the PSD obtained from the CC model compared to the von Kármán model.

With the CC model, the high frequency slope well corresponds to the measurements and therefore meets the expectations. Indeed, The estimated order ν varies between 1.16 and 1.25, so it is very different from $5/6 \approx 0.83$ the von Kármán model order. However, the CC model gain in low frequency seems to be underestimated. Consequently, the CC model works well in high frequency, but it has difficulties in estimating at low and middle frequencies.

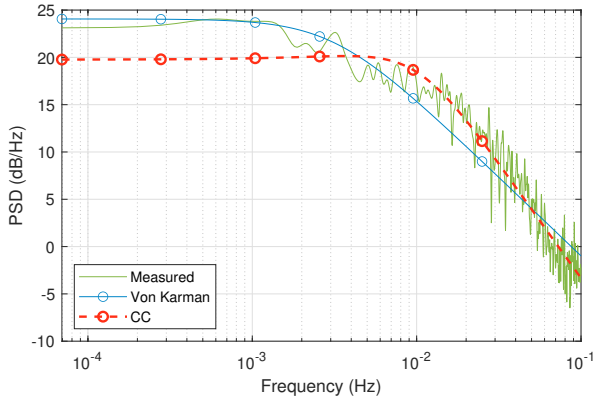

Fig. 4. Comparison between the estimated von Kármán model (–) , CC model (- -) and the measured wind PSD (–)

3.2 Improved Cole-Cole based model

To improve the CC model at low and middle frequencies, a second cell of a fractional order 2ν is added to the CC fractional function of the PSD, which will be denoted as Cole-Cole×2 (CC×2).

$$H_{CC\times 2}(s) = \frac{\sqrt{K}}{(1+(\frac{\tau_1}{2\pi}s)^{\nu})(1+(\frac{\tau_2}{2\pi}s)^{2\nu})}. \quad (17)$$

The second cell will allow the model to have a second slope in low and medium frequencies and thus a better fit. Nevertheless, the model has one more parameter to estimate and its PSD structure is more complex. Based on the PSD calculation (15)-(16) for the CC model, the PSD obtained from the CC×2 model is expressed as follows:

$$\widehat{S}_{CC\times 2}(f) = \frac{K}{D_1(f)D_2(f)} \quad (18)$$

where:

$$D_1(f) = 1 + 2\cos(\nu\frac{\pi}{2})(\tau_1 f)^{\nu} + (\tau_1 f)^{2\nu} \quad (19)$$

and

$$D_2(f) = 1 + 2\cos(\nu\pi)(\tau_2 f)^{2\nu} + (\tau_2 f)^{4\nu}. \quad (20)$$

Fig. 5 presents the PSD obtained from the CC×2 model compared to the previous proposed models.

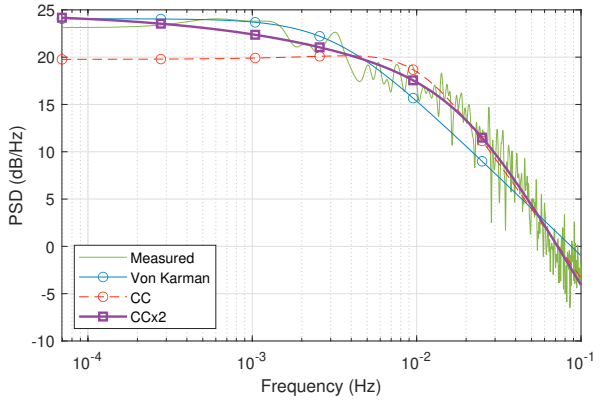

Fig. 5. Comparison between the estimated von Kármán model (–), CC model (- -) , CCx2 model (–) and the measured wind PSD (–)

For $f < 0.01$Hz, the estimated PSD of the model CC×2 has a second slope which provides a better fit as desired in middle frequencies. It can be noticed that the better fit quality in high frequency obtained with the CC model is maintained.

4. WIND MODEL DESIGN AND TIME SIMULATION

4.1 Model parameter tuning method

In this section, a methodology is presented to propose to similar models: one stemming from a black box CC×2 model, identified directly from wind measurements, and another one stemming from a grey box CC×2 model, where the parameters K, ν, τ_1 and τ_2 are obtained from direct physical parameters (namely the mean speed, the turbulence intensity and the length scale). Having this type of model is interesting in the case, where there is no access to reference measurements for the model estimation.

The estimated values of the CC×2 are presented in Fig. 6.

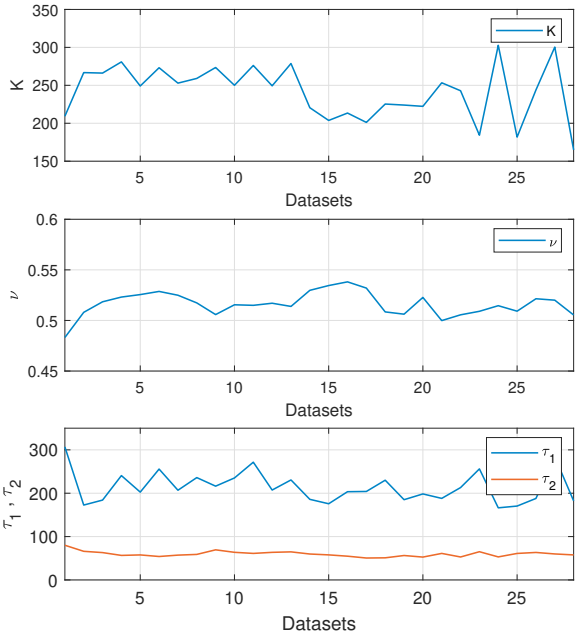

Fig. 6. Estimated parameters K, ν, τ_1 and τ_2 of the Cole-Cole×2 model for different datasets

Both CC×2 and von Kármán models well approximate the static gain, in consequence, the CC×2 model gain K is assumed to have the same expression as the von Kármán's one:

$$K = \frac{4\sigma^2 L}{\overline{V}}. \quad (21)$$

L_K is the value of the length scale is deduced from the estimated parameter K. The CC×2 model has two time constants τ_1 and τ_2. The length scale L_{12} is defined from τ_1 and τ_2, inspired by the von Kármán model:

$$L_{12} = \frac{\overline{V}\sqrt{\tau_1\tau_2}}{4.7}. \quad (22)$$

Fig. 7 shows the values of L_K and L_{12} for different datasets.

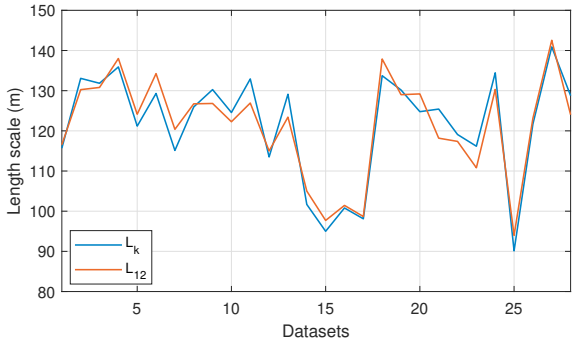

Fig. 7. Comparison between L_k the length scale value from (21) and L_{12} obtained from (22)

The obtained values of L_K and L_{12} are close to the approximated L_{ESDU} (11), therefore, the estimated model parameters do not provide aberrant values of length scale. L_K and L_{12} have the same shape, which confirms that K and time constants are related as in the von Kármán model.

Concerning the time constants, τ_1 can be calculated using the mean speed and the length scale and τ_2 can then be deduced from τ_1. Indeed, the ratio between τ_1 and τ_2 varies between 2.6 and 4.6 with an average of 3.6 (Fig. 8). Therefore, τ_2 can be approximated by:

$$\tau_2 = \frac{\tau_1}{3.6}. \tag{23}$$

This is an optimistic approximation but it allows to have consistent values for the model in the absence of a reference dataset. The equation to calculate τ_1 from the inputs becomes:

$$\tau_1 = 8.9\frac{L}{\overline{V}}. \tag{24}$$

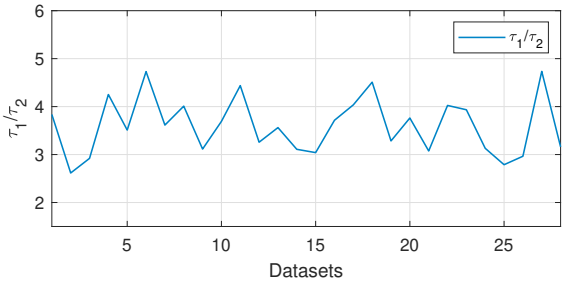

Fig. 8. Ratio between τ_1 and τ_2

Therefore, the CC×2 model parameters can be tuned using equations (21), (23) and (24) and the constants: the mean speed $\overline{V}$, the standard deviation σ and the length scale L. For the order ν, it does not vary much, so it can be fixed at the estimations mean value: $\nu = 0.516$.

4.2 CC×2 model simulation

In order to validate the methodology presented in Section 4.1, the grey box CC×2 model tuned with (21), (23) and (24) will be compared to the black box model identified in Section 3.2.

Identified black box model

The reference signal has a mean speed $\overline{V} = 6.6$m/s and a standard deviation $\sigma = 1.92$. The estimated CC×2 model parameters are:

$$K = 301.09, \quad \tau_1 = 179.17s, \quad \tau_2 = 50.13s, \quad \nu = 0.518. \tag{25}$$

The fractional transfer function of the shaping filter stemming from these parameters is:

$$H_{BlackBox}(s) = \frac{17.35}{48.72s^{1.554} + 8.59s^{1.036} + 5.67s^{0.518} + 1}. \tag{26}$$

Grey box model

Using the tuning method (see equations (21), (23) and (24)), the known inputs $\overline{V} = 6.6$m/s, $\sigma = 1.92$ and $L = 120m$, and ν fixed at the mean value of its estimations $\nu = 0.516$, the following grey box model parameters are obtained:

$$K = 269.94, \quad \tau_1 = 161.74m, \quad \tau_2 = 44.93s. \tag{27}$$

The fractional transfer function of the shaping filter issued from these parameters is:

$$H_{GreyBox}(s) = \frac{16.43}{40.7s^{1.548} + 7.62s^{1.032} + 5.34s^{0.516} + 1}. \tag{28}$$

Rational transfer functions are then drawn from (26) and (28) using the Oustaloup's approximation (Oustaloup (1983)).

PSD comparison

The PSD of the signals generated by the two models are compared to the reference data PSD (see Fig. 9).

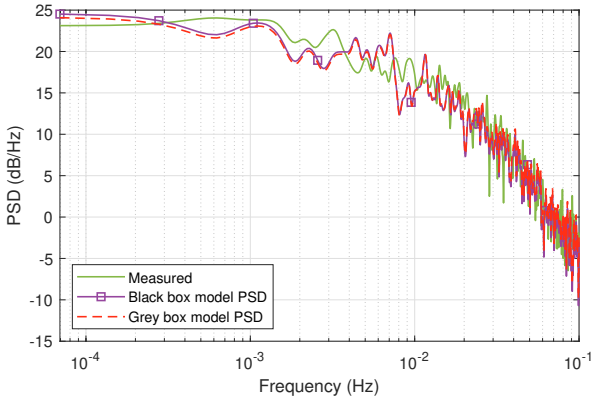

Fig. 9. Comparison between the measured wind PSD (–) , the black box CC×2 generated PSD (–) and the grey box CC×2 PSD (- -)

Both models provide signals with a PSD that has the same shape as the PSD of the wind measurements, and thus the same spectral characteristics.

5. CONCLUSION

Wind spectral characteristics are used to model turbulence because of its stochastic behavior. The von Kármán model is the reference in terms of spectral modeling of wind turbulence. However in our operating conditions, its fixed

non-integer differentiation order prevents optimal modeling in high and middle frequencies. Therefore, an improved model based on the Cole-Cole two-cell fractional functions is designed. It allows a better fit in high frequency, because it has no constraints on the differentiation order, and keeps an accurate fit thanks to the second slope brought by the second fractional order cell. Then for real-time simulation, a grey box model is proposed where the tuning parameters are similar to the von Kármán ones. A method for tuning the model parameters has been proposed for the case where there is no access to reference data. The PSD of the black box and grey box wind turbulence models showed that they have similar spectral characteristics as the measured wind. In this study, the wind mean speed was considered constant because only short-term fluctuations were studied, however the mean speed varies slowly depending on the atmospheric conditions and the season. It could be interesting to integrate a long period wind mean speed generator into the real-time wind generator.

REFERENCES

Cadalen, B., Fabien, G., Lanusse, P., Sabatier, J., and Parlier, Y. (2018a). Modelling and Control of a Tethered Kite in Dynamic Flight. *Journal of Sailing Technology*. doi:10.23919/ECC.2018.8550274.

Cadalen, B., Lanusse, P., Sabatier, J., Fabien, G., and Parlier, Y. (2018b). Robust control of a tethered kite for ship propulsion. In *European Control Conference 2018*. Limassol, Cyprus. doi:doi.org/10.5957.jst.2018.03.

Cole, K.S. and Cole, R.H. (1941). Dispersion and absorption in dielectrics i. alternating current characteristics. *The Journal of chemical physics*, 9(4), 341–351. doi: 10.1063/1.1750906.

Diop, A.D., Ceanga, E., Rétiveau, J.L., Méthot, J.F., and Ilinca, A. (2007). Real-time three-dimensional wind simulation for windmill rig tests. *Renewable Energy*, 32(13), 2268–2290. doi:10.1016/j.renene.2006.04.011.

Duhé, J.F., Victor, S., Melchior, P., Abdelmounen, Y., and Roubertie, F. (2022). Modeling thermal systems with fractional models: human bronchus application. *Nonlinear Dynamics*. doi:10.1007/s11071-022-07239-3.

ESDU (1985). 85020-Characteristics of atmospheric turbulence near the ground. Part II: single point data for strong winds (neutral atmosphere). Technical report, ESDU.

Feytout, B. (2013). *Commande crone appliquée à l'optimisation de la production d'une éolienne*. Ph.D. thesis, Université Sciences et Technologies-Bordeaux I.

Hajjem, M., Victor, S., Melchior, P., Lanusse, P., and Thomas, L. (2021). Wind fractional modeling by spectral analysis. In *2021 9th International Conference on Systems and Control (ICSC)*, 436–441. doi: 10.1109/ICSC50472.2021.9666651.

IEC (2005). Wind turbines—Part 1: Design requirements. 61400-1. Standard, International Electrotechnical Commission.

Moorhouse, D.J. and Woodcock, R.J. (1982). Background information and user guide for mil-f-8785c, military specification-flying qualities of piloted airplanes. Technical report, Air Force Wright Aeronautical Labs Wright-Patterson AFB OH.

Oustaloup, A. (1983). *Systèmes asservis linéaires d'ordre fractionnaire: Théorie et Pratique*. Masson.

Ren, G., Liu, J., Wan, J., Li, F., Guo, Y., and Yu, D. (2018). The analysis of turbulence intensity based on wind speed data in onshore wind farms. *Renewable Energy*, 123, 756–766. doi:10.1016/j.renene.2018.02.080.

Sommacal, L. (2007). *Synthèse de la fonction d'Havriliak-Negami pour l'identification temporelle par modèle non entier et modélisation du système musculaire*. Ph.D. thesis, Université Bordeaux 1.

Subrahmanyam, M.B. (1989). An extension of the simplex method to constrained nonlinear optimization. *Journal of Optimization Theory and Applications*, 62(2), 311–319. doi:10.1007/BF00941060.

van der Hoven, I. (1957). Power Spectrum of Horizontal Wind Speed in the Frequency Range from 0.0007 to 900 Cycles Per Hour. *Journal of Atmospheric Sciences*, 14(2), 160–164. doi:10.1175/1520-0469(1957)014<0160:PSOHWS>2.0.CO;2.

von Kármán, T. (1948). Progress in the Statistical Theory of Turbulence. *Proceedings of the National Academy of Sciences*, 34(11), 530 LP – 539. doi: 10.1073/pnas.34.11.530.